Collisional Viscosity of FCC Particles in a CFB

Dimitri Gidaspow and Lu Huilin
Dept. of Chemical and Environmental Engineering, Illinois Institute of Technology, Chicago, IL 60616

Particle velocity distributions were measured for a flow of 75- μm FCC particles in a CFB using a new video-digital camera technique. From the spread of particle histograms, a random oscillating particle velocity was determined. This random velocity was used to compute the powder viscosity with the help of dense-phase kinetic theory of granular flow. There was excellent agreement between this kinetic-theory measurement and previous macroscopic viscosity measurements. The dimensionless group kinematic viscosity divided by the oscillating velocity and particle diameter correlated all available data as a function of particle volume fraction.

Introduction

There exists a world-wide interest in modeling circulating fluidized beds (CFB). The development of more active fluidized cracking catalysts (FCC) for the production of gasoline from oil requires the replacement of older bubbling beds with circulating fluidized-bed units. In the electric power industry new air-pollution standards require that coal be burned in CFBs with much lower emissions of sulfur and nitrogen oxides. These requirements lead to the need for the development of predictive models for CFBs, as recently illustrated by a contest held at the 8th International Fluidization Conference in France (Knowlton et al., 1995), where modelers were asked to predict axial pressure drops and radial fluxes for FCC particles and for sand for flow in CFBs without knowing the experimental data in advance. Earlier many modeling articles were presented at the 1993 CFB conference in Pittsburgh (Avidan, 1994). Some of the predictive models require a particular viscosity as an input into the models (Tsuo and Gidaspow, 1990; Hjertager and Samuelsberg, 1992; Kuipers et al., 1992; Lyczkowski et al., 1993). Gidaspow (1994) has reviewed this theory. Good measurements of such viscosities are scarce (Schuegel, 1971; Grace, 1982; Chen et al., 1994; Miller and Gidaspow, 1992).

In the last decade a theory was developed by Savage (1983) and his collaborators, as reviewed by Gidaspow (1994), that shows how the particular viscosity can be obtained from the collision of particles. The particular kinematic viscosity is a product of the mean free path between collisions multiplied by the random oscillating-particle velocity. The mean free path is the particle diameter divided by the particle concentration. It is measured using X-ray or gamma-ray densitometers. In this study the oscillating velocity distribution was measured using a new video-digital camera technique. The dense-phase kinetic-theory viscosity agrees with the viscosity of FCC particles measured from pressure-drop shear data in the riser and with data obtained with a Brookfield viscometer. Chen et al. (1994) have previously computed such a viscosity from Campbell and Wang's (1991) solids pressure measurements. All the data for different particles sizes were correlated as a dimensionless group involving a ratio of the viscosity divided by the particle diameter and the oscillating velocity plotted vs. solid volume fraction. This plot has a minimum similar to the minimum in the dense-phase kinetic theory of gases (Chapman and Cowling, 1961).

Experimental Equipment

The experimental unit shown in Figure 1a is a two-story CFB described by Miller and Gidaspow (1992). The riser test section is an acrylic tube of 75 mm ID, with a height of 6.58 m. The particles' feed rate was controlled by a slide valve independently of the gas velocity. The particles flowing out of the riser were collected by a primary and a secondary cyclone, then recirculated through the pipeleg. The FCC particles have a density of 1,654 kg/m^3 and an average diameter 75 μm. Test positions were located at a height of 4.06 m for the dilute regime and 1.47 m for the dense regime from the bottom of the riser.

Gamma-ray and X-ray densitometers

The use of X-ray and gamma-ray densitometers for measuring particle concentrations is a well-known technique

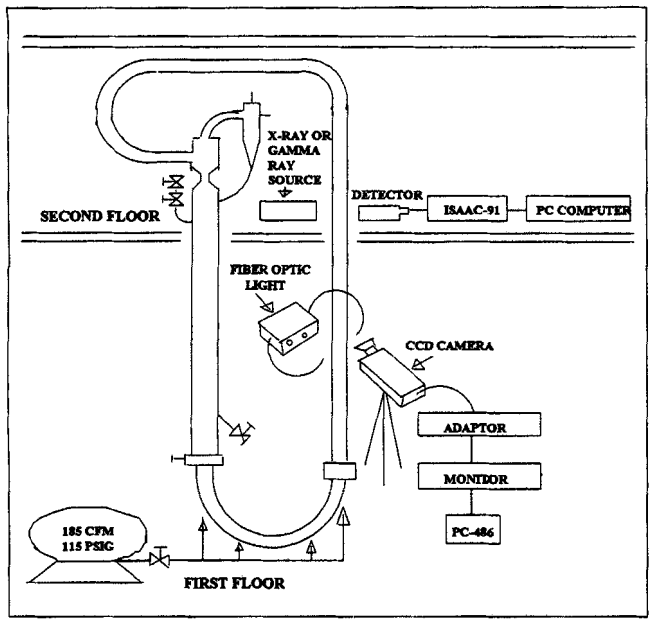

(a)

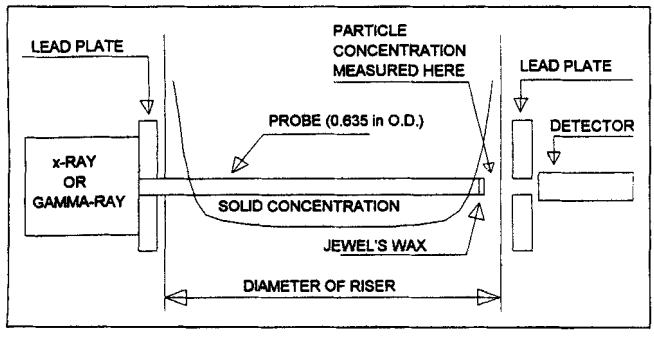

(b)

Figure 1. (a) IIT circulating fluidized bed with instruments for particle velocity and concentration measurements. (b) Sketch of determination of particle concentrations in this study (Miller and Gidaspow, 1992).

(Gidaspow, 1994). The densitometers can be used nonintrusively by rotating the source and the detector around the pipe and by constructing a complex calibration curve for deducing radial particle distributions or by means of a probe, as done by Miller and Gidaspow (1992) and in this study. Figure 1b shows a sketch of the probe extending into the pipe region. The flow conditions and the particle concentrations, as summarized in Table 1, are very similar to those already reported in this journal (Miller and Gidaspow, 1992). Visually the annular layer was seen to oscillate up and down.

Some pertinent details are as follows. The γ-ray source is a 500-Mci-Cs-137 source having a single gamma ray of 667 keV and a half-life of 30 years. The Cs-137 source was sealed in a welded stainless steel capsule. The source holder was welded, filled with lead, and provided with a shutter to turn off the

Table 1 Experimental Data (5 mm from the wall)

No.	U_g m/s	W_s kg/m^2·s	ϵ_s	U_{av} cm/s	σ_r cm/s	σ_z cm/s	θ (m/s)^2
Second Floor (4.06 m)							
1	2.89	19.03	0.0284	−18.20	19.45	198.29	1.33
2	2.89	20.89	0.0383	−31.26	15.83	213.36	1.54
3	2.89	24.33	0.0521	−52.53	23.33	258.74	2.27
4	2.89	4.380	0.0042	274.04	6.773	61.750	0.13
5	2.35	29.35	0.0924	−69.35	16.19	311.89	3.26
6	2.46	9.704	0.0025	235.35	11.49	75.928	0.21
7	2.46	20.36	0.0470	−31.02	32.78	222.22	1.72
8	2.46	29.57	0.0855	−76.02	21.08	285.38	2.74
First Floor (1.47 m)							
1	2.89	17.59	0.1355	−55.29	31.86	193.74	1.32
2	2.89	28.27	0.1959	−50.37	26.54	163.51	0.94
3	2.14	20.51	0.1591	−44.81	28.65	189.62	1.25
4	2.14	24.49	0.2114	−33.34	26.64	170.86	1.02
5	1.60	20.64	0.2146	−45.52	30.23	158.37	0.89
6	1.60	23.74	0.2407	−40.37	30.60	145.66	0.77

source. The X-ray source is a 200-mCi curium 244 source having 17.8-year half-life. This source was centered in the probe, which was a pipe of 25.4 mm diameter, sch 40 steel pipe. The cap of the pipe is covered with 1.27-cm-thick lead to prevent X-ray scatter. A 63.5-mm tube extended from the X-ray source. The intensity of the transmitted γ-ray beam was measured by using a NaI (Ti) crystal scintillation detector (Teledyne, Isotopes S-44-I/2). Another NaI crystal detector (Teledyne, Isotopes ST-44-I/B) was used for X-ray. The detector consisted of a 2-mm-thick, 5.08-cm-dia. tube with a 0.13-mm-thick beryllium window. The transmitted radiation of the γ-ray or X-ray was converted to electrical pulses by a photomultiplier (model 266, EG&G Ortec), the signals were passed through a series of data analyzers, including a preamplifier (model 778, EG&G), an amplifier, and a double-channel analyzer (DCA) (model 778). The DCA has been used to remove low-energy-level noises and produced an output logic pulse only if its amplitude falls within the energy window that is established with two preset threshold levels. The output of DCA connects to a modular data-acquisition and a control system (model Isaac-91I), which was used as the interface between the densitometer and a personal computer. In measuring local solid volume fraction, an extraction probe tube with a 6.35-mm OD was fixed at the front of the collimated lead plate. The tip of this tube was filled with jeweler's wax to prevent particles from flowing into the tube. The solid volume fraction ϵ_s is calculated as follows:

$$\epsilon_S = \frac{\ln \frac{I_o}{I} - \rho_g K_g L}{L(\rho_S K_S - \rho_g K_g)}, \tag{1}$$

where I_o and I are the intensity of incident radiation and transmitted radiation, ρ_s and ρ_g are the particle and gas density, respectively, and K_s and K_g are the mass attenuation coefficients of particles and gas, respectively. The solid volume fraction is calculated directly from a plot of the natural logarithm of intensity, since all other components of the equation are constant after calibration with a full and an empty tube, as described in great detail by Seo and Gidaspow (1987).

High-resolution microimaging/measuring system

The high-resolution microimaging/measuring system for the particle-velocity measurements consists essentially of two units: a high-resolution microimage system and a data-managing system (see Figure 1). The high-resolution microimage system is a 2/3-in. (17-mm) color video camera (DXC-151A) that uses a charge coupled device (CCD), a solid-stage image sensor. This camera has ten electronic shutter settings and four modes for gain control. The horizontal resolution of the camera is 460 TV lines, and it has a sensitivity of 2000 lux at 0 dB for gain. The camera adapter is a Sony CMA-D2, which connects the camera to a 486/33-MHz IBM computer. The personal computer has a microimaging board and a microimaging software, Image-Pro Plus, for data measurement and analysis. Bahary (1994) demonstrated this technique for gas–liquid–solid fluidization (Gidaspow et al., 1995b).

For good visualization of the microscopic movement of particles, a fiber-optic light was used. The area of view in most experiments was a 5×20 mm. As the particles were fluidized inside the riser, the camera with a zoom lens, 18–108 mm, and close-up focus transferred its field of view into the monitor. Figure 2 shows a typical streak made by the particles. These streak lines represent the distance traveled by the particles in a given time interval specified on the camera. The images were then captured and digitized by the Image-Pro Plus software. To obtain reliable velocity information, the time between exposures must be selected so as to obtain a sufficient displacement to achieve an acceptable velocity resolution, but must not be so large that the particle moves out of the field of view. The local velocity is then estimated from the equation

$$u = \frac{\Delta L(x,y)}{\Delta t}. \tag{2}$$

Two-dimensional velocity components, radial and vertical, are determined.

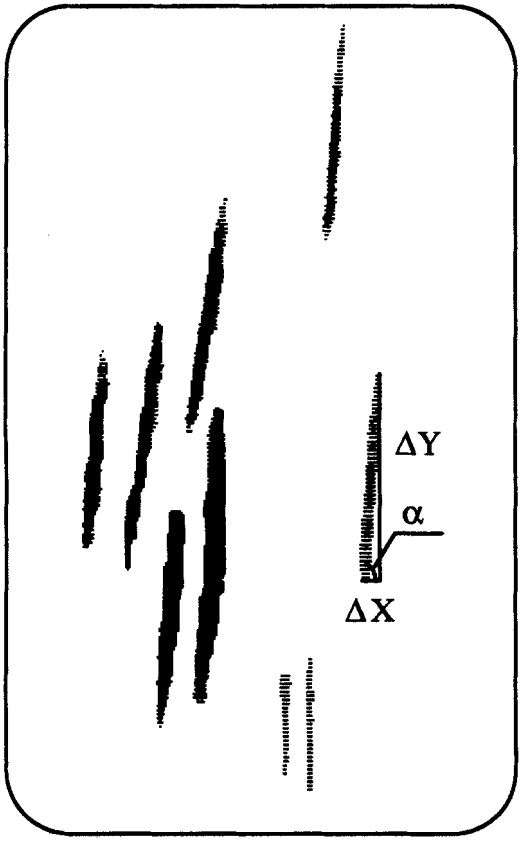

Figure 2. Streak images captured by the CCD camera recording system for flow of 75 μm FCC particles in the IIT CFB.

This figure shows a small portion from screen on which images are captured, for example, $\Delta y = 1.44$ mm; $\Delta x = 0.22$ mm; $\alpha = 80°$; $\Delta t = 0.5$ ms. Velocity is negative when streak is formed moving down on the computer monitor.

Particle-Velocity Distributions and Granular Temperature

Typical particle speed, axial, and radial velocity distributions are shown in Figure 3a, 3b, and 3c, respectively. The ordinate, expressed in $(\text{cm/s})^{-1}$, is the probability that the velocity will fall within the indicated velocity range. It is obtained by dividing the number of particles in the velocity range shown by the total number of measurements and by the velocity in the indicated velocity range. For example, see Gidaspow (1994), fig. 10.10. Velocities are negative when the particles flow down, as visually observed.

The mean particle speed and velocity are calculated as the arithmetic average. The standard deviations were calculated based on the instantaneous velocity of particles from mean values:

$$\sigma = \frac{1}{N} \sum_{i=1}^{N} \sqrt{(v_i - v_m)^2}, \tag{3}$$

where v_i and v_m are instantaneous particle velocity and mean particle velocity, respectively. Shao et al. (1995) have used a similar procedure to calculate the fluctuating velocity using a laser Doppler anemometer.

The granular temperature, θ, is calculated, assuming the angular and the radial velocity fluctuations to be equal as

$$\theta = \frac{1}{3}(\sigma_r^2 + \sigma_\theta^2 + \sigma_z^2) = \frac{2}{3}\sigma_r^2 + \frac{1}{3}\sigma_z^2. \tag{4}$$

Table 1 summarizes the data measured in this study.

Radial particle and granular temperature profiles

Under dilute conditions, for a flux of 4.2 $\text{kg/m}^2\text{-s}$, the digital camera technique allows a measurement of radial velocity distributions. Figures 4 and 5 show the particle speed and granular temperature distributions. The profiles are not symmetrical, as in the experiments of Miller and Gidaspow (1992). For higher particle concentrations, data reported in Table 1 were obtained about 5.0 mm from the wall.

Particulate viscosity

Using the kinetic theory of granular flow, one can calculate the solid viscosity in terms of particle properties, solid vol-

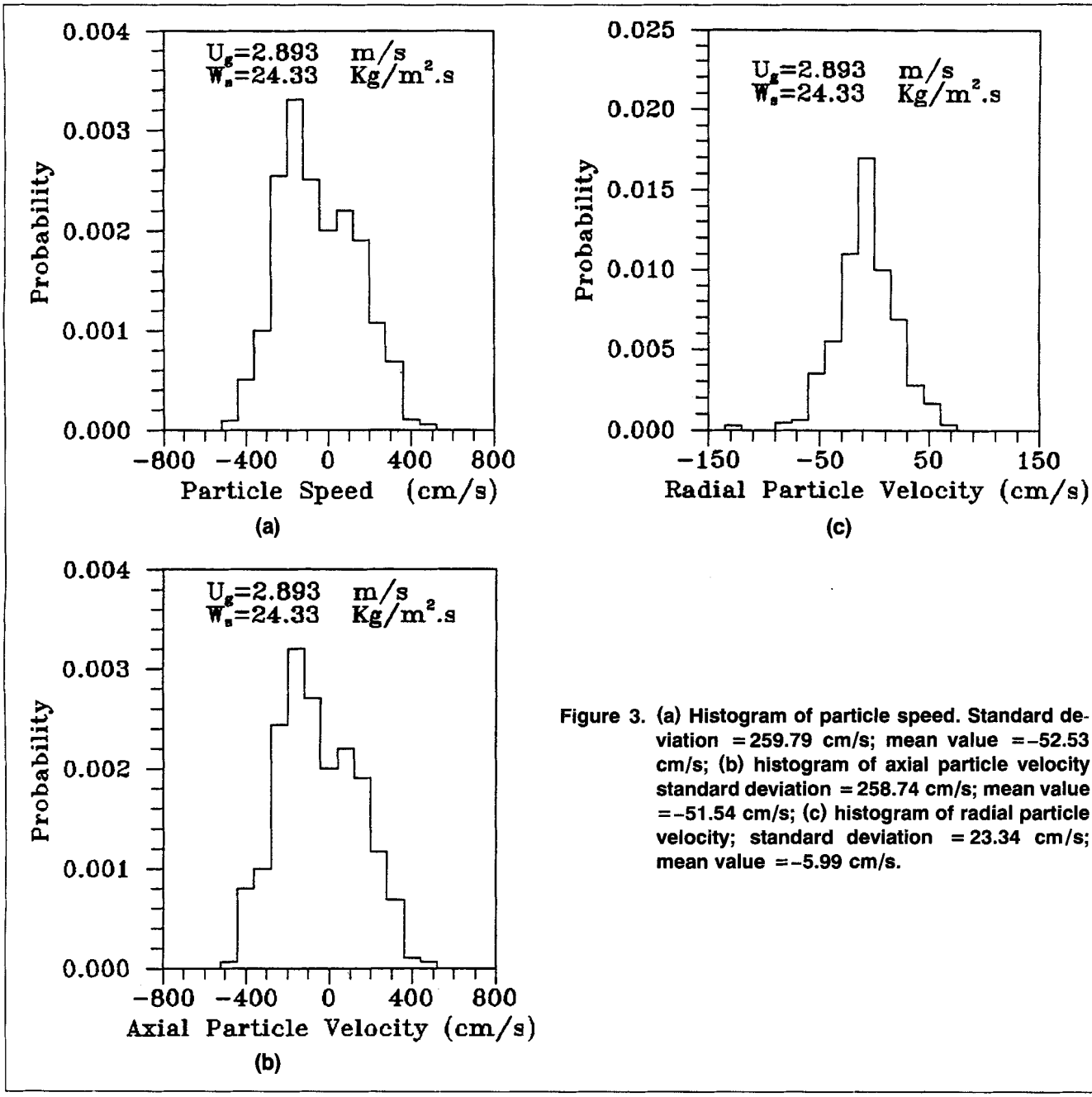

Figure 3. (a) Histogram of particle speed. Standard deviation = 259.79 cm/s; mean value = −52.53 cm/s; (b) histogram of axial particle velocity standard deviation = 258.74 cm/s; mean value = −51.54 cm/s; (c) histogram of radial particle velocity; standard deviation = 23.34 cm/s; mean value = −5.99 cm/s.

ume fraction, and granular temperature. The following relationship for solid viscosity was derived by Gidaspow (1994):

$$\mu_s = \frac{5\rho_s d_p\sqrt{\pi\theta}}{48(1+e)g_o}\left[1+\frac{4}{5}(1+e)g_o\epsilon_s\right]^2 + \frac{4}{5}\epsilon_s^2\rho_s d_p g_o(1+e)\left(\frac{\theta}{\pi}\right)^{0.5}, \quad (5)$$

where g_o is the radial distribution function and θ the granular temperature. A nearly identical equation was derived in a pioneering paper by Lun et al. (1984). Chen et al. (1994) showed how the solid viscosity can be computed from the measurement of solid pressure, which is related to the granular temperature by means of the equation of state for particles. Shao et al. (1995) showed how to calculate this viscosity from the direct measurements of granular temperature obtained with a laser Doppler velocity meter.

Equation 5 can be interpreted as (Gidaspow, 1994):

kinematic viscosity = mean free path × random oscillating velocity.

The mean free path depends on particle concentration, while the granular temperature was measured in this study. The restitution coefficient, e, is nearly unity in our experiment.

Figure 6 shows the granular temperature obtained in this study and a comparison of computed granular temperature

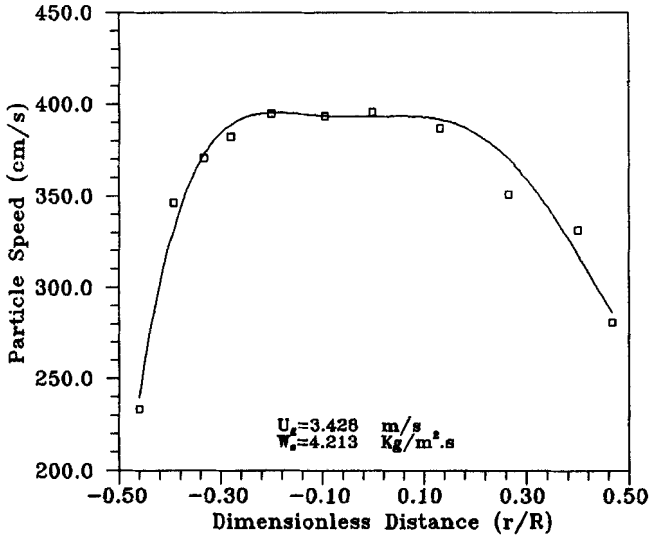

Figure 4. Averaged particle speed vs. radial distance in the dilute region.

of other investigations. In this plot, Miller and Gidaspow's (1992) viscosity data were converted to the granular temperature using Eq. 5. Campbell and Wang's (1991) pressure data were converted to the granular temperature using the equation of the state for particles:

$$p_s = \epsilon_s \rho_s \theta [1 + 2\epsilon_s (1+e) g_o] \tag{6}$$

$$g_o = \left[1 - \left(\frac{\epsilon_s}{\epsilon_{s,max}}\right)^{1/3}\right]^{-1}. \tag{7}$$

Figure 6 shows that granular temperature rises sharply with solid volume fraction in the dilute region, reaches a maximum at a volume fraction of solid of about 10%, and then decreases.

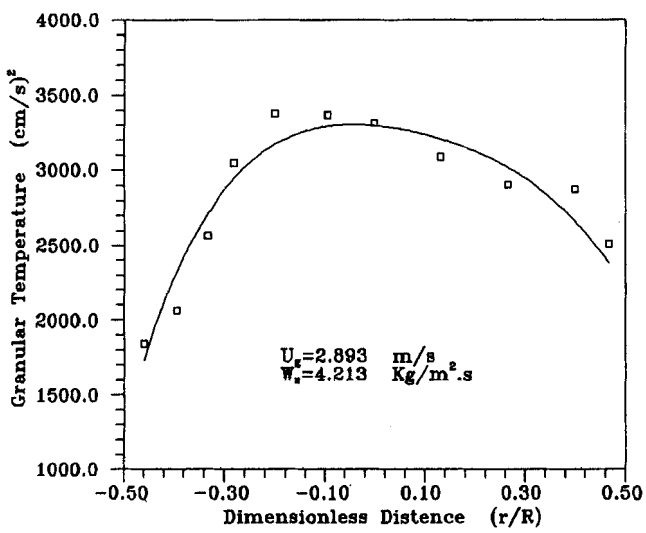

Figure 5. Granular temperature vs. radial distance in the dilute region.

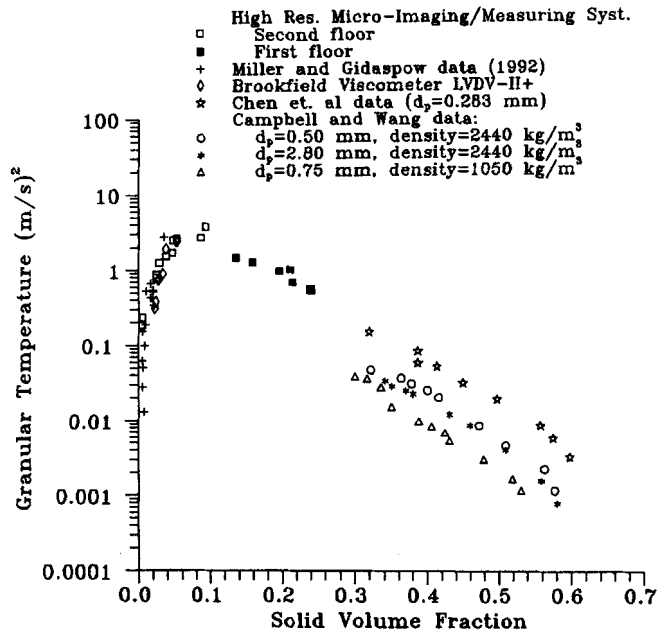

Figure 6. Measured and computed granular temperature.

Measurements are in Table 1. Campbell and Wang's and Chen et al.'s pressure data converted to granular temperature using Eq. 6; Miller and Gidaspow's viscosities converted to granular temperature using Eq. 5.

Figure 7 shows a comparison of the viscosity obtained by three different methods: (1) by calculation using Eq. 5 and the granular temperature obtained in this study; (2) from Miller and Gidaspow (1992) viscosity obtained from a pressure-drop balance using radial velocity distributions; (3) by a Brookfield viscometer immersed in the riser. The Brookfield viscometer method is described in Bahary (1994). In view of experimental errors, there is excellent agreement between these measurements. The kinetic theory method shows that the viscosity is caused by particle oscillations.

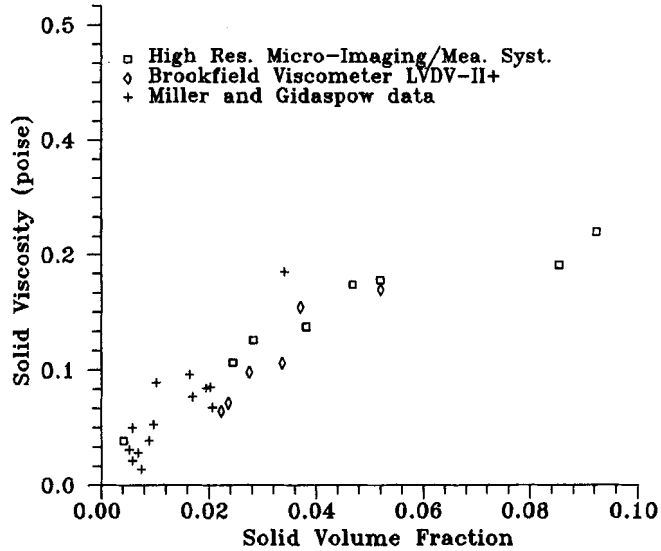

Figure 7. FCC powder viscosity measured in three different ways.

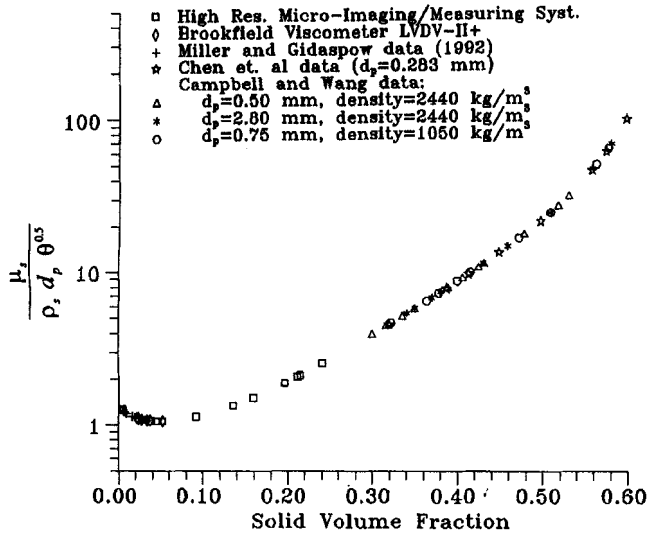

Figure 8. Dimensionless solid viscosity correlation.

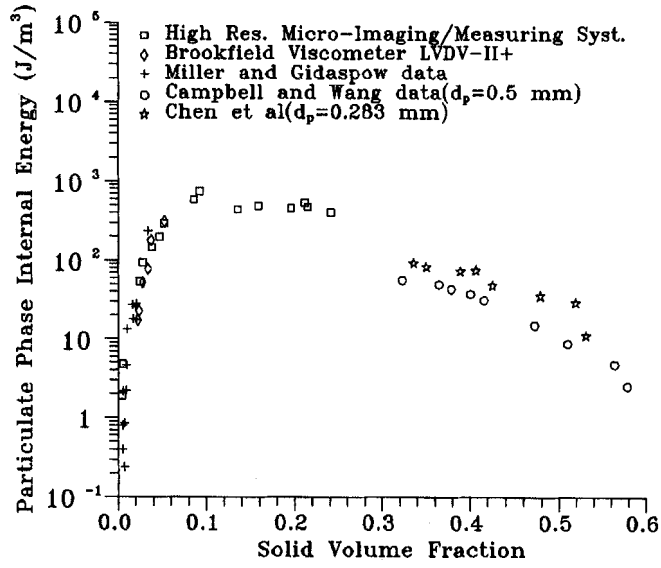

Figure 9. Kinetic (translational) portion of powder internal energy.

Figure 8 shows that data for different particle sizes can be correlated by means of a dimensionless group related to that found in the dense-phase kinetic theory of gases (Chapman and Cowling, 1961). The minimum is at a solid volume fraction of 0.057.

The difference between the gas-kinetic and the particulate-kinetic theories is that the latter depends upon the granular temperature, which is related to the particle velocity. Theoretically the granular temperature can be obtained from a kinetic energy balance (e.g., Sinclair and Jackson, 1989). For example, for dense flow (Gidaspow, 1994), the granular temperature depends upon shear rate as follows:

$$\theta = \frac{1}{15(1-e)}\left(\frac{\partial u_s}{\partial y}\right)^2 d_p^2. \tag{8}$$

For low particulate velocities, as found in liquid–solid and three-phase fluidized beds (Bahary, 1994), low values of granular temperature were measured. Hence, Eq. 5 gives lower μ_s. Thus our earlier relation (Miller and Gidaspow, 1992)

$$\mu_s = 5\epsilon_s \text{(poise)} \tag{9}$$

cannot be considered universal.

Computed Particle Internal Energy and Frequency

Analogous to the gas theory, the knowledge of granular temperature allows one to calculate the internal energy. The particulate-phase internal energy with oscillations in three-dimensions can be computed from the simple equation given by Gidaspow (1994):

$$U = C_v \epsilon_s \rho_s \theta, \tag{10}$$

where the specific heat C_v was 3/2.

Figure 9 displays the results of the calculations. These values of energy are of order of one-tenth the particle suspending energy shown in Figure 10.

The energy required for suspending the particles per unit volume is

$$N_{\text{sus}} = [\epsilon_s \rho_s + (1-\epsilon_s)\rho_g]hg \approx \epsilon_s \rho_s hg. \tag{11}$$

Figure 11 shows the particle collision frequency as a function of solid volume fraction in bubbling and circulating fluidized beds calculated according to following equation (table 9.1 of Gidaspow, 1994):

$$f_{\text{coll}} = 6.77\left(\frac{\epsilon_s}{d_p}\right) g_o \sqrt{\theta}. \tag{12}$$

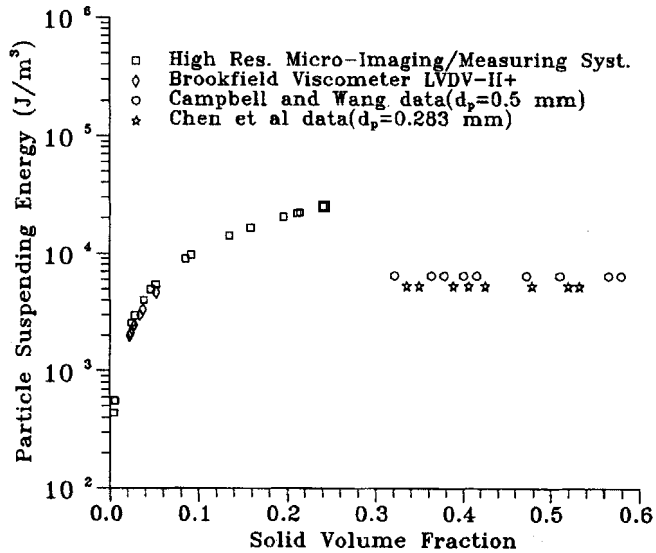

Figure 10. Particle suspending energy for circulating and bubbling fluidized beds.

For Campbell and Wang and Chen et al. curve, bed height in Eq. 11 was not well known.

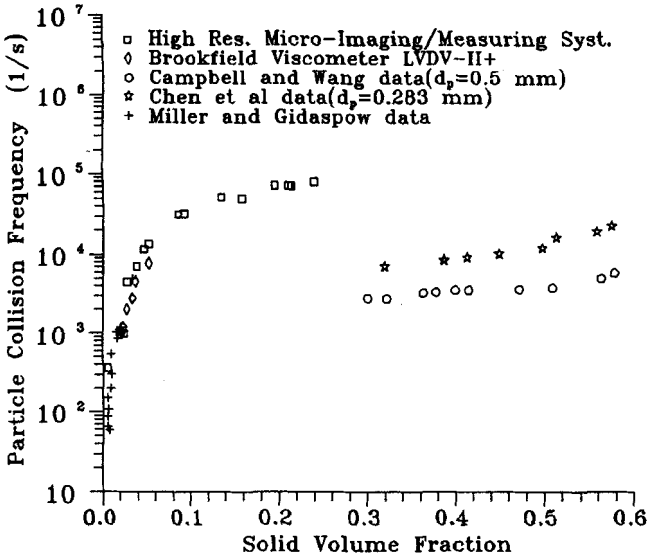

Figure 11. Particle collision frequency in bubbling and circulating fluidized beds.

Granular temperature in Eq. 12 was estimated from pressure data for Campbell and Wang and Chen et al.

It can be seen that the range of particle collision frequency is about 10^2 to 2×10^4. There appear to be fewer collisions in a bubbling bed. Direct verification of the number of collisions is desirable. Note that this collision frequency is still very high compared with the bubbling frequency, which is of the order of 2 Hz. Hence the fluidized-bed oscillations consist of two types: high-frequency oscillations computed here, and low-frequency oscillations measured with a gamma densitometer (Gidaspow et al., 1995a).

Conclusions and Discussion

1. Miller and Gidaspow (1992) have obtained viscosities of FCC particles from a time-averaged laminar-type momentum balance on the particles. Such a balance is valid for the volume fraction of particles greater than a one-tenth of a percent, since for dense mixtures the gas properties can be neglected compared with the solid properties. For example, the mixture Reynolds number does not involve the gas properties (Gidaspow, 1994). The Reynolds number $Re_{\text{mixture}} = (\epsilon_s \rho_s D_{\text{pipe}} v)/\mu_s$. Typical values of this Re_{mixture} range from 10 to 100. Hence for dense mixtures, the gas turbulence in a pipe without particles has no relation to flow of the dense mixture. The viscosity was calculated from a balance of Newtonian shear at the core–annular interface and pressure drop minus the core weight of particles. The physical interpretation of the viscosity calculated by Miller and Gidaspow (1992) is the same as that of the viscosity of a gas. The kinetic-theory-type measurements presented in this article verify that the FCC viscosity is due to the collision of the particles.

2. Reliable values of FCC viscosities are needed for numerical simulation and design improvements of catalytic crackers. There are no handbook values available of such viscosities. We used the viscosity relation of Miller and Gidaspow (1992) to predict the flux and concentration profiles in a riser for the contest held at the 1995 International Fluidization Conference in France. We successfully predicted the unexpected observed maxima in fluxes. A quote from the review of the hydrodynamics of CFB risers (Berruti et al., 1995) is as follows: "The best type III model (hydrodynamic) was created by Gidaspow and Sun which matched some significant trends in the radial mass flux profiles."

3. The collapse of viscosity data shown in Figure 8 computed from measurements of granular temperature and granular pressure by Chen et al. and by Campbell and Wang for different particle sizes indicates that the equation of state for particles, Eq. 6, is valid. Indeed in a submitted article we experimentally show that for FCC particles there exists an analogue of the equation of state for an ideal gas. The second term in Eq. 6 is a van der Waals-type correction. The present theory does not as yet have the cohesive force constant in the van der Waals equation.

4. We show that the internal energy of the powder, that is, the energy of oscillation, is a significant portion of the energy required to suspend the powder. Hence the acoustic behavior of the mixture is strongly affected by particle concentration. It is known that the stability of ballistic missiles is enhanced by aluminum particles present in the propellant (Pape et al., 1996).

5. In the CFB the granular temperature shown in Figure 6 rises sharply as the collision frequency depicted in Figure 11 increases with particle concentration. Beyond a volume fraction of particles of 0.1 the granular temperature decreases as the mean free path of particles decreases with the rising particle concentration. This decrease of granular temperature with a decrease of the mean free path is well established theoretically. For example, see eq. (10.20) in Gidaspow's (1994) book. Work in progress shows that such a behavior holds for liquid–solid and three-phase fluidized beds (Gidaspow et al., 1995b). The present theory does not, however, fully explain the sharp rise in granular temperature due to a singularity at zero solids volume fraction.

Acknowledgment

This work was supported by National Science Foundation Grant CTS-9305850.

Notation

d_p = particle diameter
L = distance
h = bed height
N_{sus} = particle suspending energy
U_{av} = average particle speeds
U_g = superficial gas velocity
W_s = solid mass flux

Literature Cited

Avidan, A. A., "Circulating Fluidized Bed Technology IV," *AIChE Proc. Int. Conf. on Circulating Fluidized Beds*, Pittsburgh, (1993).

Bahary, M., "Experimental and Computational Studies of Hydrodynamics in Two and Three Phase Fluidized Beds," PhD thesis, Illinois Inst. of Tech., Chicago (1994).

Berruti, F., J. Chaouki, L. Godfroy, T. S. Pugsley, and G. S. Patience, "Hydrodynamics of Circulating Fluidized Bed Risers: A Review," *Can. J. Chem. Engi.*, **73**, 579 (1995).

Campbell, C. S., and D. G. Wang, "Particle Pressures in Gas Fluidized Beds," *J. Fluid Mech.*, **227**, 495 (1991).

Carlos, C. R., and J. F. Richardson, "Solids Movement in Liquid Fluidized Beds: I. Particle Velocity Distribution," *Chem. Eng. Sci.*, **23,** 813 (1968).

Chapman, S. and T. G. Cowling, *The Mathematical Theory of Non-Uniform Gases*, 2nd ed., Cambridge University Press, Cambridge, (1961).

Chen, J. C., W. Polashenski and K. Tuzla, "Normal Solid Stress in Fluidized Beds," AIChE Meeting, San Francisco (1994).

Gidaspow, D., R. Bezbaruah, and J. Ding, "Hydrodynamics of Circulating Fluidized Beds: Kinetic Theory Approach," *Fluidization VII*, O. E. Potter and D. J. Nicklin, eds., Engineering Foundation, New York, p. 75 (1992).

Gidaspow, D., "Multiphase Flow and Fluidization, Continuum and Kinetic Theory Descriptions," *Academic Press*, New York (1994).

Gidaspow, D., L. Huilin and A. Therdthianwong, "Measurement and Computation of Turbulence in a Circulating Fluidized Bed," International Fluidization Conf., Tours, France (1995a).

Gidaspow, D., M. Bahary, and Y. Wu, "Hydrodynamic Models for Slurry Bubble Column Reactors," AIChE Meeting, Miami Beach, FL (1995b).

Grace, J. R., "Fluidized-Bed Hydrodynamics," *Handbook of Multiphase Systems*, G. Hetsroni, ed., Hemisphere, (1982).

Hjertager, B. H., and A. Samuelsberg, "Computer Simulation of Flow Processes in Fluidized Bed Reactor," *KONA Powder Particle*, **10,** 96 (1992).

Knowlton, T. M., J. Matsen, and D. Geldart, "Benchmark Modeling Experiment," International Fluidization Conference, Tours, France (1995).

Kuipers, J. A. M., K. J. van Duin, F. P. H. van Beckum, and W. P. M. van Swaaij, "A Numerical Model of Gas-Fluidized Beds," *Chem. Eng. Sci.*, **47,** 1913 (1992).

Lun, C. K. K., S. B. Savage, D. J. Jeffrey, and N. Chepurniy, "Kinetic Theories for Granular Flow, Inelastic Particles in Couette Flow and Singly Inelastic Particles in a General Flow Field," *J. Fluid Mech.*, **140,** 223 (1984).

Lyczkowski, R. W., I. K. Gamwo, F. Dobran, Y. H. Ali, B. T. Chao, M. M. Chen, and D. Gidaspow, "Validation of Computed Solids Hydrodynamics and Pressure Oscillations in a Bubbling Atmospheric Fluidized Bed," *Powder Technol.*, **76,** 65 (1993).

Media Cybernetics Inc., *High Resolution Micro-Imaging/Measuring System, Operating Manual*, Silver Spring, MD (1993).

Miller, A., and D. Gidaspow, "Dense, Vertical Gas-Solid Flow in a Pipe," *AIChE J.*, **38,** 1801 (1992).

Pape, R., D. Gidaspow, and Steven Wu, "Multiphase Flow in Slurry Bubble Column Reactors and Solid Propellant Rockets," ASME Int. Symp. on Numerical Methods for Multiphase Flows, San Diego (1996).

Savage, S. B., *Granular Flows at High Shear Rates, Theory of Dispersed Multiphase Flow*, R. E. Meyer, ed., Academic Press, New York, (1983).

Schuegel, K., "Rheological Behavior of Fluidized Systems," *Fluidization*, J. F. Davidson and D. Harrison, eds., Academic Press, New York (1971).

Seo, Y., and D. Gidaspow, "An X-Ray-Gamma-Ray Method of Measurements of Binary Solid Concentrations and Voids in Fluidized Beds," *Ind. Eng. Chem.*, **26,** 1622 (1987).

Shao, S., H. J. Slovik, and H. Arastoopour, "The Flight Time Technique for Simultaneous Measurements of Particle Flow Parameters using a Laser Doppler Anemometer (LDA)", Int. Fluidization Conf., Tours, France (1995).

Sinclair, J. L., and R. Jackson, "Gas-Particle Flow in a Vertical Pipe with Particle-Particle Interaction," *AIChE J.*, **35,** 1473 (1989).

Sony Corporation, *Sony CCD Color Video Camera Operating Manual*, Tokyo, Japan (1993).

Tsuo, Y. P., and D. Gidaspow, "Computation of Flow Patterns in Circulating Fluidized Beds," *AIChE J.*, **38,** 885 (1990).

Manuscript received July 19, 1995, and revision received Feb. 2, 1996.